



Article

Biocomposite Materials Based on Chitosan and Lignin: Preparation and Characterization

Elena Rosova ^{1,2,*}, Natalia Smirnova ^{1,2}, Elena Dresvyanina ², Valentina Smirnova ¹, Elena Vlasova ¹, Elena Ivan'kova ^{1,2}, Maria Sokolova ¹ , Tatiana Maslennikova ³, Konstantin Malafeev ², Konstantin Kolbe ^{1,2}, Mikko Kanerva ⁴  and Vladimir Yudin ^{1,2}

- ¹ Institute of Macromolecular Compounds, Russian Academy of Sciences, V.O. Bolshoi Pr. 31, 199004 St Petersburg, Russia; nvsmirnova@hq.macro.ru (N.S.); ves@hq.macro.ru (V.S.); spectra@imc.macro.ru (E.V.); imc@hq.macro.ru (E.I.); pmarip@mail.ru (M.S.); kkolbe@hq.macro.ru (K.K.); yudinve@gmail.com (V.Y.)
- ² Institute of Biomedicine Systems and Biotechnology, Peter the Great St Petersburg Polytechnic University, Polytechnicheskaya Street 29, 195251 St Petersburg, Russia; tms@spbstu.ru (E.D.); malafeev_kv@spbstu.ru (K.M.)
- ³ Grebenshchikov Institute of Silicate Chemistry, Russian Academy of Sciences, Makarova Emb. 2, 199034 St Petersburg, Russia; maslennikova@iscras.ru
- ⁴ Materials Science and Environmental Engineering, Tampere University, P.O. Box 589, FI-33101 Tampere, Finland; mikko.kanerva@tut.fi
- * Correspondence: rosova@hq.macro.ru; Tel.: +79-21-311-3575



Citation: Rosova, E.; Smirnova, N.; Dresvyanina, E.; Smirnova, V.; Vlasova, E.; Ivan'kova, E.; Sokolova, M.; Maslennikova, T.; Malafeev, K.; Kolbe, K.; et al. Biocomposite Materials Based on Chitosan and Lignin: Preparation and Characterization. *Cosmetics* **2021**, *8*, 24. <https://doi.org/10.3390/cosmetics8010024>

Academic Editor: Maria Beatrice Coltelli

Received: 20 February 2021

Accepted: 16 March 2021

Published: 22 March 2021

Publisher's Note: MDPI stays neutral with regard to jurisdictional claims in published maps and institutional affiliations.



Copyright: © 2021 by the authors. Licensee MDPI, Basel, Switzerland. This article is an open access article distributed under the terms and conditions of the Creative Commons Attribution (CC BY) license (<https://creativecommons.org/licenses/by/4.0/>).

Abstract: In this study, bioactive composite systems based on natural polymers (chitosan and lignin) were prepared in this study. The structural, mechanical, and morphological properties of chitosan-based materials containing various amounts of lignin filler were investigated. The infrared IR spectroscopy data confirmed the formation of chemical bonds between the components of the obtained composites. The mechanical properties of film samples were studied in air and in physiological solution. It was demonstrated that the breaking elongation values of the obtained film samples in the wet state were higher (150–160%) than the corresponding (average) value of a pure chitosan film (100%). The scanning electron microscopy and atomic force microscopy data demonstrated that the introduction of lignin had caused significant changes in the surface morphology of films. The appearance of a strongly pronounced texture and porosity facilitated cell proliferation on the surface of composites, i.e., the bioactivity of film samples was enhanced with an increasing lignin content in the chitosan matrix.

Keywords: biocomposite; chitosan; lignin; composite matrix; dermal fibroblasts; tissue engineering

1. Introduction

Among the main tasks of tissue engineering is the development of artificial biomedical constructions that include (i) cells able to form functional and viable extracellular matrix; (ii) an appropriate biodegradable carrier (matrix) for cell transplantation; (iii) bioactive molecules (cytokines and growth factors), which stimulate the regeneration of cells of damaged tissues [1,2]. The main criteria for the selection of a carrier material are absence of toxicity, biodegradability, and biocompatibility.

The most suitable polymers for tissue engineering purposes that meet the above-mentioned requirements are polysaccharides, polylactide, and composites based on these polymers [3,4]. The preparation of polysaccharide composites with fillers with various morphologies and particle sizes as well as the introduction of plasticizers into a matrix polymer makes it possible to adjust the mechanical and other properties of proper material [5,6]. The resulting composites either possess a combination of properties inherent to their components or acquire some new properties (if components interact with each other in any way) [7]. The necessary requirements for fillers include adhesive compatibility with

the applied polymeric matrix [8], biocompatibility, and bioresorbability. The use of natural fillers (such as chitin nanofibrils [5], collagen [9], or starch [10]) enables one to obtain a non-toxic, biocompatible, and biodegradable material system.

The interaction between the surface of a tissue engineering matrix and biological molecules is the most important aspect in designing biomaterials and the governing factor for their efficient use. The determining factors for efficient cellular processes (proliferation and differentiation) are the hydrophilicity of biomaterial and the structure of free surface, which interacts with cells (in terms of roughness, morphology, and surface charge). Among the main requirements for novel tissue engineering materials is sufficient mechanical strength (ability to provide support and transport of transplanted cells), and the possibility of using them in humid or liquid media.

Chitosan is a linear polysaccharide possessing a number of unique properties (biocompatibility, absence of toxicity, biodegradation ability, and antimicrobial); due to chitosan characteristics, it is widely used in medicine, pharmaceuticals, and cosmetology [11–13]. However, chitosan-based materials have one considerable drawback that prevents their utilization in the design of tissue engineering constructions. Chitosan swells strongly in liquid media, which leads to the significant deterioration of its mechanical characteristics [14]; changes in surface morphology; and, as a consequence, this drawback has a negative influence on cell adhesion and proliferation on the chitosan surface [15]. Several authors have suggested modifying chitosan properties by the addition of lignin. In addition to cellulose and proteins, lignin is among the most common natural polymers and attracts considerable attention from researchers, including those engaged in biomedicine [16–18].

Lignin is natural irregular amorphous polymer consisting of phenylpropane structural units [19]. It contains virtually all known oxygen-containing organic functional groups, which determine its reactivity. It has been established that lignin possesses enhanced sorption properties, and thus it is used for binding various microorganisms, endogenous and exogenous toxins, heavy metal ions and radioactive isotopes. Lignin is employed as an active component and filler in preparation of various composite systems. Several recent studies have showed that lignin is suitable for manufacturing package films of thermoplastic polymers due to its antioxidant properties [20,21].

The authors of a current work [22] described the preparation of biodegradable films based on chitosan and lignin that may be used as package and wound dressing materials. Chitosan/lignin composites are used in the production of bioplastic [21]. The authors of a recent work [23] developed chitosan/lignin composites with improved physico-chemical properties capable of the sorption of toxic organic compounds and metal ions; these materials can be applied to reduce constantly growing industrial water pollution. Chitosan/lignin composites possess antimicrobial activity against Gram-positive and Gram-negative bacteria [24], and thus can be used in the development of food packaging materials. The authors of a research [25] developed biopolymeric materials based on the lignin/chitosan complex, which possess high thermostability, mechanical strength, capability for controlled moisture sorption, and antimicrobial properties. The lignin composite materials are promising for the production of medicinal and hygienic products.

In the search for a new generation of biomedical materials, lignin has attracted significant interest due to its promising characteristics. Lignin has been proved to be suitable for biomedical applications, such as tissue engineering scaffolds, biocompatible antibacterial agents, and release materials in drug delivery systems. The most significant characteristics of lignin and its derivatives are antioxidant activity, inherent antibacterial activity, adhesiveness, biodegradability, biocompatibility, favorable stiffness, high thermal stability, and low cost [26]. Owing to these unique properties, lignin-based materials are promising for a wide range of biomedical applications. Lignin may be used in combination with other polymers to obtain composites with improved functionalities.

There are no literature data on the biological activity of chitosan/lignin composites. However, it may be suggested that these composites will demonstrate bioactivity and biofunctionality due to the natural properties of their components. In this connection, the

preparation and study of chitosan/lignin composites is an actual task in medicine-related research. In the present work, we prepared chitosan/lignin composite films with various percentages of the additive, studied structural and morphological features of the obtained film samples, their mechanical properties, and bioactivity.

2. Materials and Methods

2.1. Preparation of Films

We used crab chitosan obtained from Biolog Heppe GmbH (Landsberg, Germany) (MM = 148 kDa, deacetylation degree 86.5%), and technical hydrolysis lignin (THL) (brown powder) produced by Kirovsk Biochemical Plant in accordance with the Russian State Standard Specification 18,300.

THL was obtained by industrial percolation with diluted acid hydrolysis of softwoods. THL was sieved to obtain a fraction of 0.25 mm (retained between the sieves of 0.25 and 0.50 mm, THL0.25 mm). These lignin particles were additionally grounded in a rotary-jet mill OMICRON 60 (New Technol. Disperse Systems, St. Petersburg, Russia) to obtain a fraction of approximately 5 μ m (weight-median-diameter as analyzed by Laser Particle Sizer ANALYSETTE 22 MicroTec plus (Fritsch, Idar-Oberstein, Germany), THL5 μ m). The hydrothermal treatments (HTA) were carried out under alkaline conditions (5% NaOH) in an autoclave at 220 °C for 2 h. The basic idea behind the HTA was the transformation of insoluble THL into soluble product with low M_w , which was free of concomitant polysaccharides, ash, and extractives. The molecular weight was \approx 1000 Da, as determined by size-exclusion chromatography. Structural characterization carried out by employing tandem electrospray ionization-mass spectrometry and 1D and 2D nuclear magnetic resonance spectroscopy revealed that upgraded lignins are oligomers (trimers-pentamers) with highly degraded propane chains and possess polyconjugated condensed aromatic structures [27,28].

The initial chitosan films were prepared by casting chitosan solutions in acetic acid onto glass supports. A weighed amount of chitosan (1.5 g) was dissolved in 0.1 M acetic acid. The solution was stirred for 24 h, then filtered using a Schott filter glass and degassed. The cast solutions were exposed in air at room temperature until drying was complete. The resulting films were removed from glass supports and treated with a 1 M solution of NaOH to transfer chitosan into the base form.

To prepare composite films, a calculated weighed amount of lignin was dissolved in water under vigorous stirring for 48 h at room temperature. The insoluble fraction, according to the manufacturer's information, was less than 10%. Then, concentrated acetic acid and chitosan were successively added to lignin solution under stirring until a concentration of 1.5% was reached for the chitosan solution in 0.1 M acetic acid. The final mixture was stirred for 24 h at 20 °C. The resulting solution was filtered through a Shota-100 filter, degassed using a water-jet pump, then cast on a glass dish and dried in air at room temperature. The mass ratio of chitosan—lignin in the solution was 1.5:0.15; 1.5:0.30 and 1.5:0.45 (10%, 20%, and 30%, respectively). The resulting films were homogeneous, transparent, smooth, and characterized by brown color of lignin. An increase in the lignin content in the composite led to a more intense color of the film.

The chitosan film series (casting from chitosan/acetic acid solution) and chitosan/lignin composite film series were treated with 1 M NaOH. The treatment time with NaOH was 30 min. Then the films were washed with water.

2.2. Studies of Film Structure

The structures of the obtained films were studied by spectral and microscopic methods. The infra-red IR spectra were obtained using a Vertex 70 spectrometer (Bruker) equipped with attenuated total reflectance (ATR) microattachment ("Pike"), which contained ZnSe internal reflection element. During registration of ATR spectra, the correction for penetration depth depending on wavelength was made.

An X-ray structural analysis (WAXD) was performed with the aid of a DRON-3M diffractometer (“Burevestnik” Research and Production Association) in the reflection mode (the Bragg–Brentano geometry); Cu K_{α} irradiation was used ($\lambda = 1.54183 \text{ \AA}$, nickel β -filter). The samples were placed into quartz cuvettes; no averaging rotation was applied. The diffractograms were registered in the step regime in the angular range $2\theta = 5\text{--}50$ grad with a step size of 0.02 grad; the exposure time at each working point was 1 s. The processing of the obtained data and peak identification were performed using the DFWin.

The structure of the obtained materials and cell–material interaction was analyzed using a Supra 55 VP electron microscope (Carl Zeiss, Jena, Germany). Prior to the experiments, a gold layer with a thickness of about 25 nm was deposited onto the samples in an Eiko-IB3 Ion Coater; the ion current was 6 mA, and the voltage was 5 kV across the electrodes.

Statistical Data Analysis. The reproducibility of the data was demonstrated by analyzing all experimental and control groups in triplicates. The data were presented by an average value and (plus minus) standard error (SEM). For the statistical analysis, a Student’s t-test was used. The differences were considered significant at $p < 0.05$.

Atomic force microscopy (AFM) studies were performed using a SPM-9700HT scanning probe microscope (Shimadzu, Kyoto, Japan). The AFM images were taken in air at room temperature. The instrument operated in the force modulation mode, and an FMR-10 Silicon tip (tip radius less than 10 nm) was employed. Image resolution was 512×512 points.

2.3. Studies of Swelling

The kinetics of swelling of the initial chitosan films and composite systems were studied in distilled water and a physiological solution at a room temperature until the swelling–time curve reached a plateau.

The swelling degree was determined gravimetrically and calculated by the following formula:

$$Q = (m - m_0)/m_0, \quad (1)$$

where m and m_0 are the masses of swollen and dry films, respectively.

2.4. Studies of Mechanical Properties

Mechanical parameters (tensile strength, Young’s modulus or stiffness, breaking elongation) were measured for the obtained film samples in the dry and wet states. The mechanical properties of the dry samples were determined with the aid of an Instron 5943 universal testing machine; the base length was 20 mm, and extension rate was 10 mm/min. Before measurements, films were kept in a desiccator at a relative air humidity of 66% for not less than 24 h. The wet samples were tested in a Biss Ligagen biobath filled with physiological solution using an Instron ElectroPulse E1000 setup. The base length was 10 mm, and film width was 2 mm. The extension rate was 5 mm/min. The wet samples were tested at $37 \pm 1 \text{ }^{\circ}\text{C}$. Before the measurements, the samples were exposed to the medium for about 5 min. Additionally, all the characteristics determined for the wet samples in a biobath were preliminarily measured in the dry state using the same Instron ElectroPulse E1000 setup.

The temperature dependences of the storage modulus (E') and mechanical loss tangent ($\tan\delta$) of the chitosan films were studied by dynamic mechanical analysis using a DMA 242C/1/F setup (Netzsch, Germany). The measurements were conducted at a frequency of 1 Hz, the heating rate was $5^{\circ}/\text{min}$, and the amplitude of film sample deformation was 0.1%.

2.5. Analysis of Biocompatibility of Materials

Human dermal fibroblasts were obtained from the collection of cell cultures of Institute of Cytology, RAS (St Petersburg, Russia). The cells were cultured in Dulbecco modified Eagle medium (DMEM) supplemented with 1% of penicillin, 1% of streptomycin, 1% of

fungizone, 2 mM of L-glutamine, and 10% of fetal bovine serum (FBS). The cells were incubated at 37 °C in a humidified atmosphere containing 5% of CO₂. For the experiments, fibroblasts from pre-confluent cultures were harvested with 0.25% of trypsin/EDTA. Trypsin was neutralized with FBS, and the cells were re-suspended in DMEM (all Thermo Fisher Scientific, Waltham, MA, USA).

The studies of cell viability and proliferation on the composite films were performed using the MTT test. The film matrices were placed in 24-well plates, and culture medium was added. Sterilized silicone rings were placed on top to keep the scaffolds submerged, and 25 × 10³ fibroblasts were seeded on top of the scaffolds. The cells were resuspended in culture medium and then incubated in a humidified atmosphere containing 5% of CO₂. After 4 days of incubation, the culture medium was removed, and each well was treated with 10 µL of 3-(4,5-dimethylthiazol-2-yl)-2,5-diphenyl tetrazolium bromide (MTT) (Thermo Fisher Scientific, USA), 5 mg/mL in culture medium, and incubated for 4 h at 37 °C in a humidified atmosphere containing 5% of CO₂. The yellow MTT was reduced to blue-purple formazan in the presence of the mitochondrial dehydrogenase. This enzyme is present in intact living cells; hence, the produced blue-purple color should be proportional to the number of viable cells. The MTT solution was then replaced with 100 µL/well of dimethylsulfoxide (DMSO, Paneco Ltd., Moscow, Russia) to dissolve the formazan salts; upon slow agitation for 10 min, a blue-purple solution was formed. The absorbance of this solution was measured at 570 nm using a SPECTROstar[®] nano microplate reader for absorbance measurements (BMG LABTECH, Ortenberg, Germany).

3. Results

3.1. Dynamic Mechanical Analysis

Dynamic mechanical analysis (DMA) is the most informative method for the investigation of the phase composition of polymeric composite films [29]. The method is based on the temperature dependency of the storage modulus (E') and loss modulus (E'') of a polymer-based material sample. The method allows one to determine temperatures of phase and relaxation transitions, particularly, glass transition temperatures (T_g) of polymers. DMA also makes it possible to estimate the thermodynamic compatibility of the components of a two-phase system. When components are thermodynamically compatible, the T_g value of a composite differs from that of individual polymers. When two polymers are incompatible, two glass transition temperatures typical of individual components are observed.

The determination of chitosan glass transition is discussed in several studies [30–33]. The authors of a work [30] used thermogravimetric analysis (TGA) and DMA to study the structure and thermal properties of chitosan films; it was demonstrated that the glass transition temperature of chitosan in the base form is 250–260 °C.

According to a research [34], the glass transition temperature of lignin varies from 110 to 150 °C and depends on the sample origin (raw material) and its molecular mass.

Figure 1 presents the temperature dependences of storage modulus E' and mechanical loss tangent ($\tan\delta$) for the studied films. The $\tan\delta$ (T) curve obtained for chitosan in the base form contained two wide maximums: $T_1 = 80\text{--}100$ °C and $T_2 = 250\text{--}270$ °C. The first maximum ($T_1 = 80\text{--}100$ °C) typical of chitosan films is related to the removal of adsorbed water. The second maximum ($T_2 = 254$ °C) is presumed to be attributed to the glass transition temperature of chitosan in its base form [30].

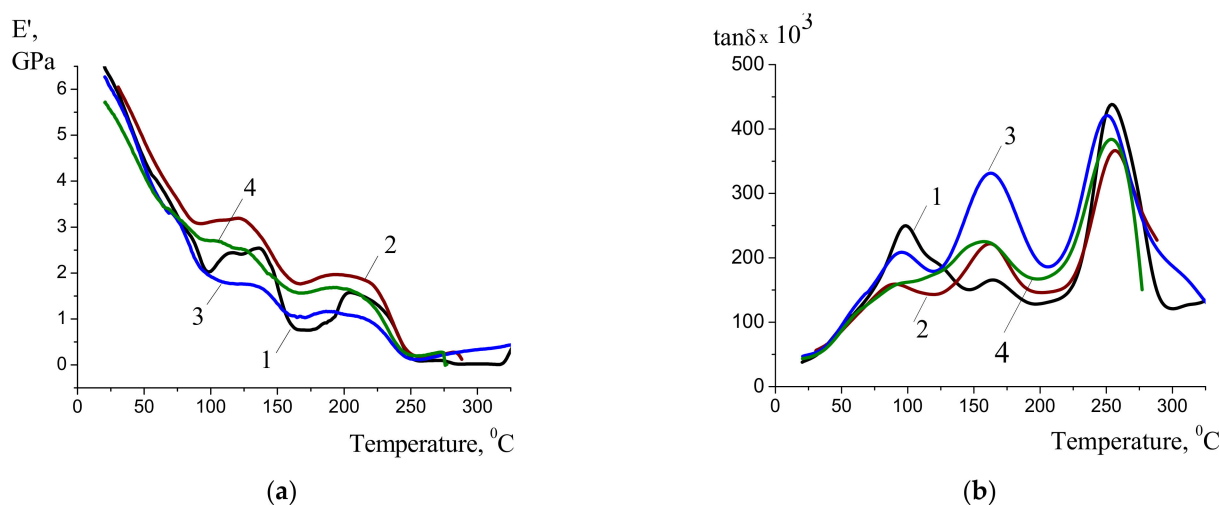


Figure 1. Temperature dependences of storage modulus E' (a) and $\tan\delta$ (b) for pure chitosan film (1) and chitosan-based composite films containing 10% (2), 20% (3), and 30% (4) of lignin.

The behaviors of the $E'(T)$ and $\tan\delta(T)$ curves obtained for the composite films containing 10, 20, and 30 wt% of lignin were different to the pure chitosan. A wide maximum at $T = 162\text{--}167\text{ }^{\circ}\text{C}$ appeared in the $\tan\delta(T)$; most probably, this peak is related to the lignin glass transition. The chitosan maximum ($T_2 = 254\text{ }^{\circ}\text{C}$) was retained for all the studied composite films. This leads to the conclusion that the composite films (where chitosan is present in the base form) containing 10–30% of lignin have a two-phase structure, i.e., the studied polymers are thermodynamically incompatible.

3.2. IR Spectroscopy

In order to reveal the type of interaction between chitosan and lignin, IR spectroscopy studies of the films were carried out. The IR spectrum of chitosan film in the base form (Figure 2) contained the following absorption bands: a wide band at $3500\text{--}3100\text{ cm}^{-1}$ (primary and secondary OH groups), two bands at 3450 and 3310 cm^{-1} attributed to NH_2 groups, a band at 3282 cm^{-1} assigned to the valence vibrations of NH groups, a characteristic amide absorption band near 1650 cm^{-1} (Amide I), a complex band at 1570 cm^{-1} including the Amide II band (1550 cm^{-1}), and a band related to non-protonated NH_2 groups of chitosan at 1580 cm^{-1} . The lignin spectrum contained the following characteristic bands: a wide band near $3500\text{--}3100\text{ cm}^{-1}$ related to aromatic and aliphatic OH groups, a band at 1710 cm^{-1} assigned to vibrations of $\text{C}=\text{O}$ in the carboxylic group, and bands of the aromatic ring near 1600 and 1500 cm^{-1} .

The IR spectra of chitosan-based composite films containing 10 to 30 wt% of lignin did not contain the band attributed to the $\text{C}=\text{O}$ bond of the carboxylic group (1710 cm^{-1}). However, a shoulder appeared at 1556 cm^{-1} on the 1570 cm^{-1} band; this shoulder might be attributed to carboxylate ion. Thus, it may be assumed that the carboxylic group in lignin and the chitosan amino group formed a salt [35–37].

In the spectrum of the composite containing 10 wt% of lignin, intensities of the peaks at 1067 and 1030 cm^{-1} became considerably higher, which is presumed related to the formation of hydrogen bonds. The hydroxyl group present in the lignin phenolic ring may interact with the 1,4-glycoside oxygen atom of chitosan [22].

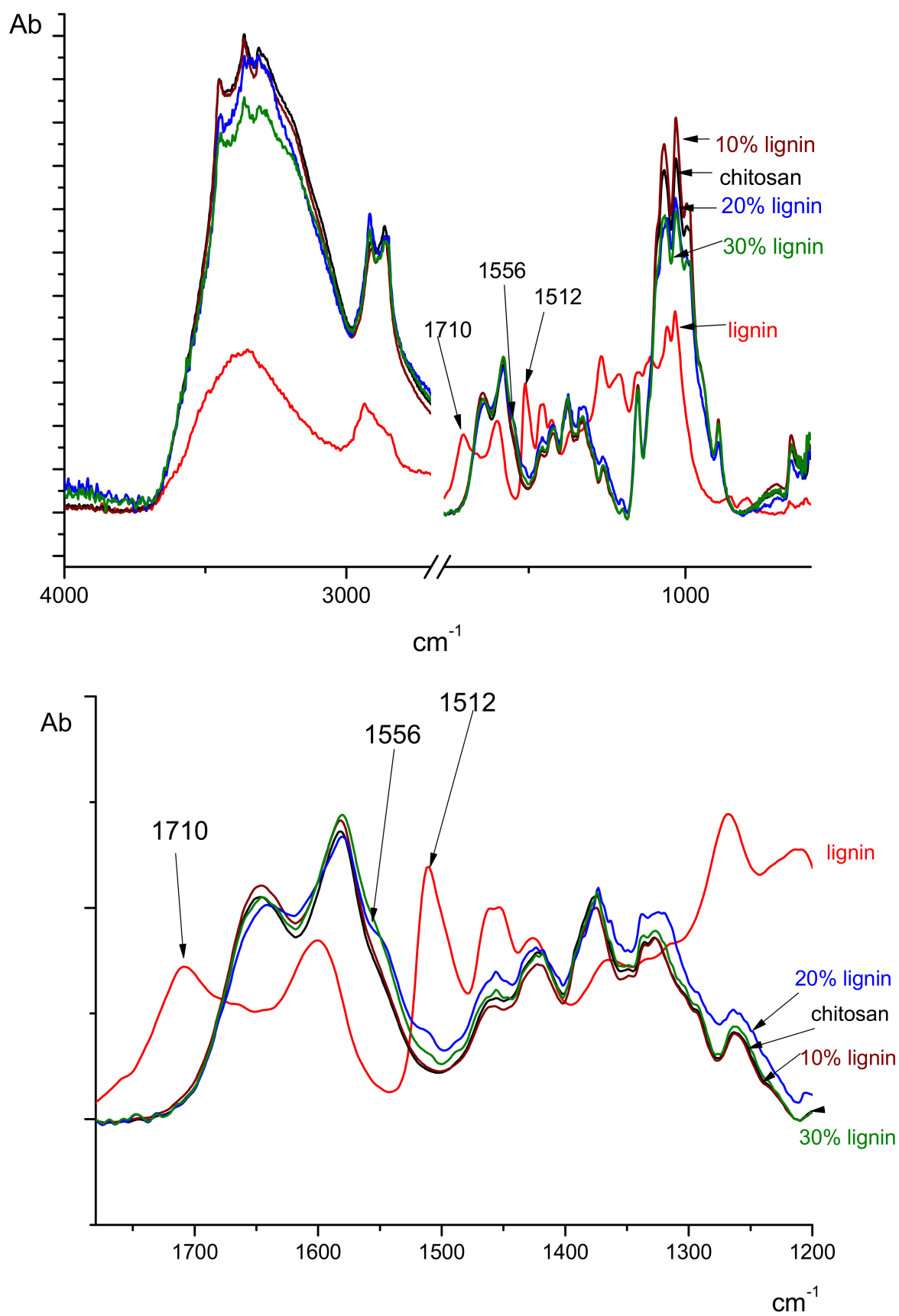


Figure 2. The IR spectra of lignin, chitosan film, and composite films containing 10%, 20%, and 30% of lignin.

3.3. X-Ray Structural Analysis

Figure 3 presents the WAXD patterns of chitosan and the composites containing various amounts of lignin. It is seen that the pattern for chitosan in the base form contained three diffraction maximums at $2\theta = 10.5^\circ$, 15.3° , and 20.5° (values of interplanar distances $d = 8.45 \text{ \AA}$, 5.84 \AA , and 4.39 \AA , respectively), which agrees with the data presented in the literature [38]. The presence of both peaks at $2\theta = 10.5^\circ$ and 15.3° confirms the presence of hydrated and anhydrous forms of chitosan in the films, respectively [39,40]. The introduction of lignin into chitosan led to an amorphization of the films. Additionally, the peaks at $2\theta = 10.5^\circ$ were more pronounced, while the peaks at $2\theta = 15.3^\circ$ were weaker for composite films in comparison with the initial chitosan. This suggests the increasing content of hydrated forms and decreasing content of anhydrous forms with lignin addition.

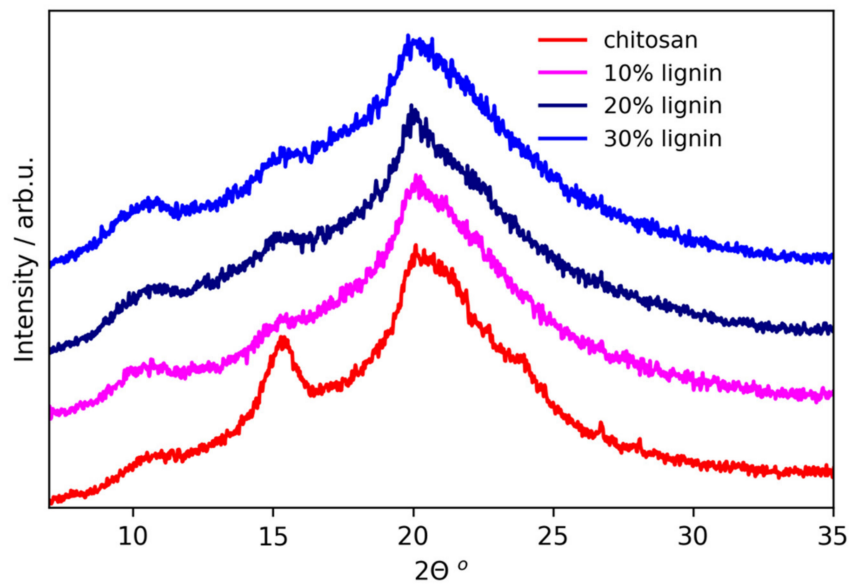


Figure 3. The WAXD patterns of the chitosan film and composite films with different contents of lignin.

3.4. Scanning Electron Microscopy (SEM)

The results of the SEM studies demonstrated that the pure chitosan film had a smooth flat surface (Figure 4a). Lignin here is composed of agglomerates containing irregular-shaped particles (Figure 4d). The surface morphology of composites differed from that of the initial chitosan and lignin film samples. The presented images show that the composites had textured porous surfaces. With an increasing lignin content in the samples, the texture's scale and number of pores also increased.

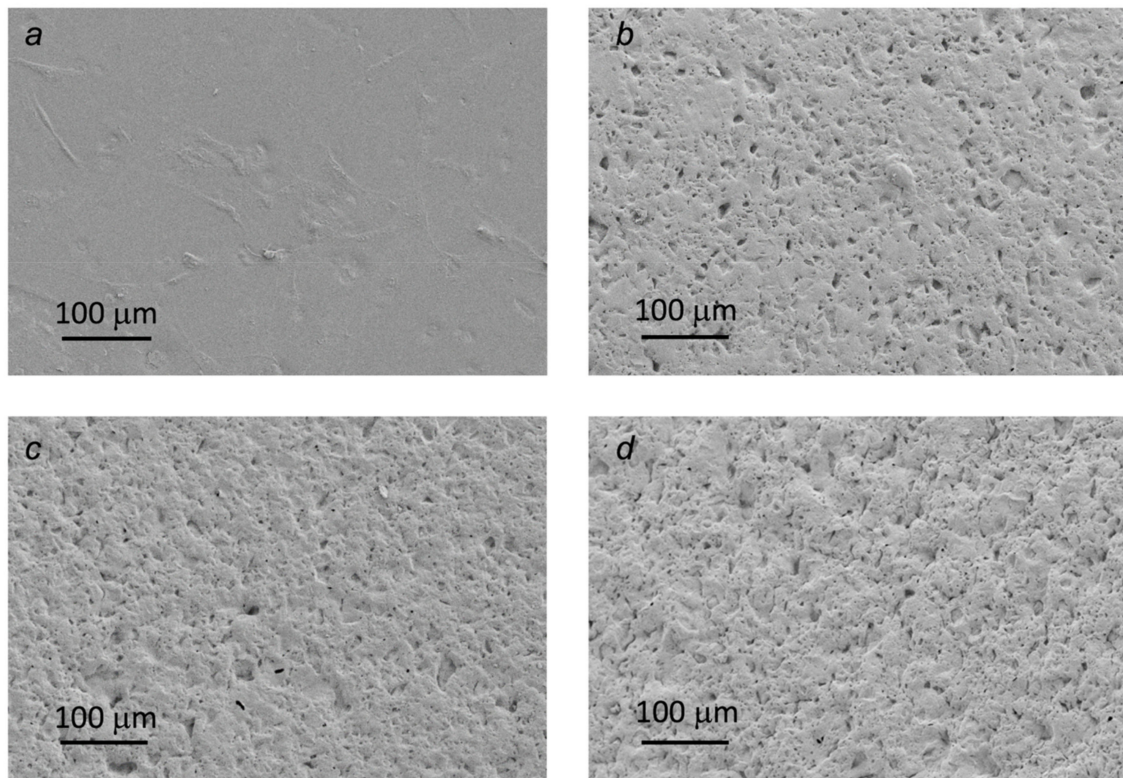


Figure 4. SEM micrographs of the pure chitosan film (a); composite films containing 10% (b), 20% (c), and 30% of lignin (d).

3.5. AFM Studies

AFM images of the samples under study are given in Figure 5. The analysis of the AFM images of the initial chitosan film showed a rather uniform morphology (Figure 5a) with granules of 100–200 nm in size. The introduction of 10% of lignin resulted in an increase in roughness (R_q) from 12 to 50 nm with minor changes in morphology (Figure 5b). A further increases in the lignin content up to 20 and 30% (Figure 5c,d, respectively) led to the tremendous increase in the sizes of structural elements (up to several microns) accompanied by an increase in roughness up to $R_q = 201$ and 125 nm, respectively. Additionally, the introduction of 30% of lignin resulted in the appearance of submicron sized holes, which can be beneficial for cell adhesion.

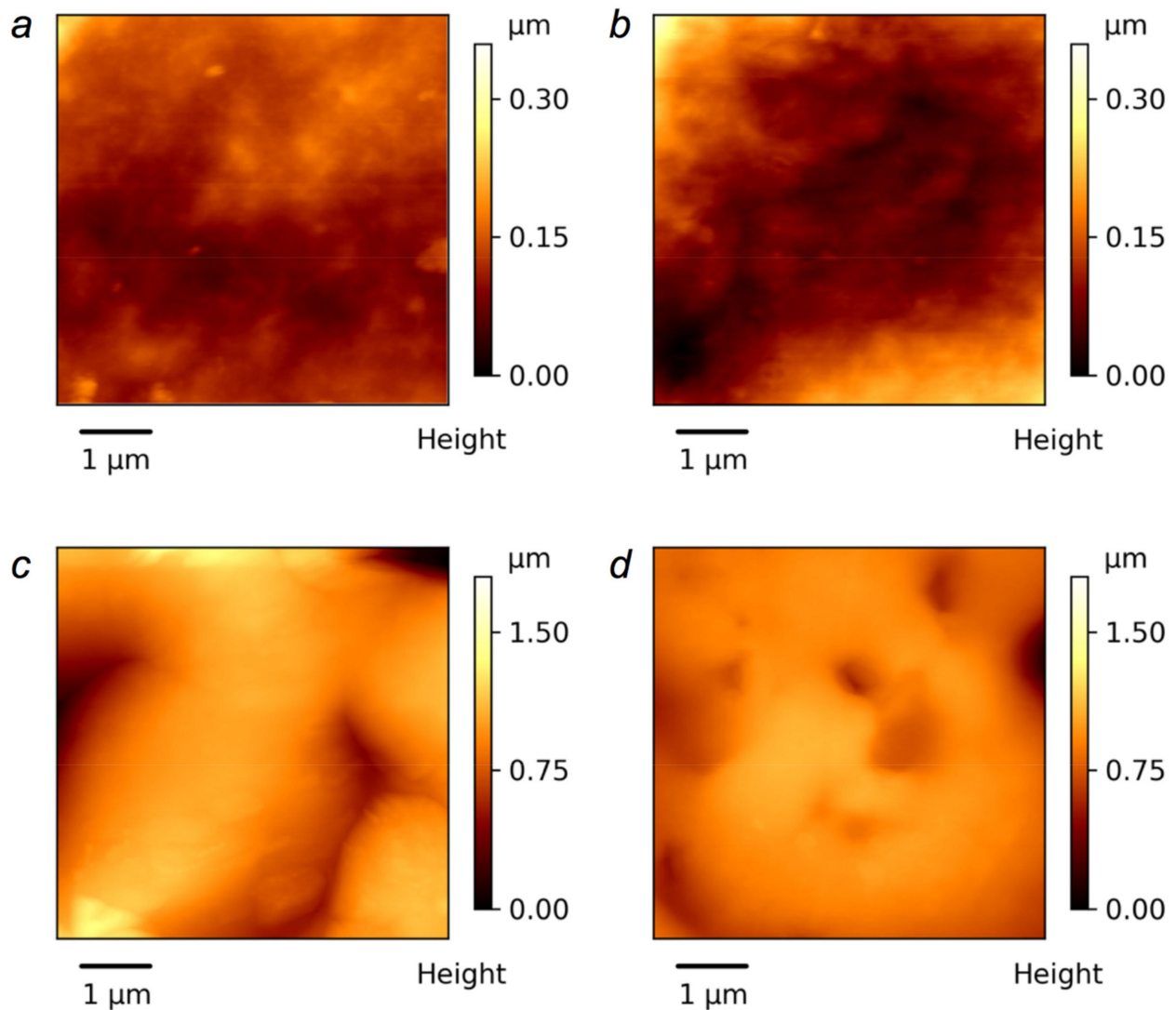


Figure 5. The AFM images of the unmodified chitosan film (a) and composite films with different lignin contents: 10% (b), 20% (c), and 30% (d).

3.6. Swelling of Films

The swelling of the samples was studied in water and a physiological solution at a room temperature. Both in water and in the physiological solution, all samples were stable and retained their mechanical integrity throughout the experiment. For all the samples, the maximum degree of swelling was insignificantly higher in the physiological solution (1.2–1.5 g/g) (Figure 6b), while in water, this value was equal to 1.0–1.2 g/g (Figure 6a). The highest swelling degree in both solvents was found for the initial chitosan films, and among the composites, the highest value was demonstrated by the system containing the largest amount of lignin. The lowest degree of swelling in both media was found for the samples containing 10% of lignin.

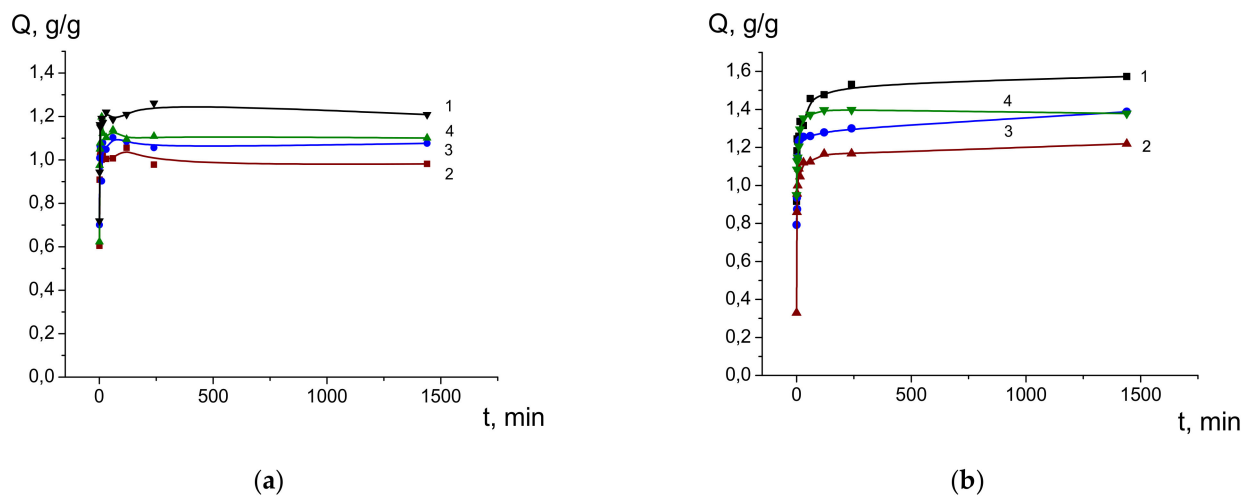


Figure 6. The swelling of films in water (a) and in a culture medium (b): 1—chitosan; 2—the composite containing 10% of lignin; 3—the composite containing 20% of lignin; 4—the composite containing 30% of lignin.

3.7. Mechanical Properties

The mechanical characteristics of the pure chitosan films and composite films in the dry state (such as strength, Young's modulus, and breaking elongation) were determined in the uniaxial extension regime; the sample base length was 20 mm. The data presented in Table 1 show that the introducing of lignin into the chitosan matrix led to an insignificant decrease in the strength and modulus of composite films; these parameters virtually did not depend on the lignin content in a composite films. At the same time, the breaking elongation of composite films was almost two times lower than that of the initial chitosan film; this characteristic does not depend on the lignin percentage either.

Table 1. Mechanical properties of the studied films in the dry state determined using an Instron 5943 universal testing machine with the sample base length of 20 mm.

Composition	Strength, MPa	Modulus, GPa	Breaking Elongation, %
chitosan	75.21 ± 18.3	3.11 ± 0.4	21.45 ± 11.4
chitosan + 10% lignin	53.41 ± 4.5	2.75 ± 0.2	9.4 ± 2.2
chitosan + 20% lignin	54.26 ± 3.8	2.79 ± 0.3	9.36 ± 2.4
chitosan + 30% lignin	54.5 ± 5.5	2.84 ± 0.3	8.83 ± 3.3

Similar results were obtained during the testing of the films with the aid of an ElectroPulse E1000 setup (base length 10 mm; see Table 2). The studies also revealed that the modified films had slightly lower mechanical strength in the wet state than the pure chitosan film, and this parameter did not depend on filler percentage. Thus, for the pure chitosan film, the mechanical strength decreased from 62 ± 5 MPa (dry state) to 27 ± 3 (wet state); for the composite film containing 10% of lignin, the loss of strength was less significant (from 36 ± 3 in the dry state to 25 ± 2 MPa in the wet state). Similarly, for the rest of composite films, this strength loss in the wet state (in comparison with that in the dry state) did not exceed 20% (Table 2). The breaking elongation for wet films was considerably higher than that in the dry state: for the pure chitosan films, it rose from $45 \pm 10\%$ to $101 \pm 1\%$, and for the lignin-containing films, the difference was even higher (from 27–30% to 155–160%). Meanwhile, the value of breaking elongation for composite films (both in the dry and wet states) did not depend on filler amount and was virtually similar for all samples.

Table 2. Mechanical characteristics of chitosan films and their composites; sample base length: 10 mm.

Sample	Chitosan		Chitosan + 10% Lignin		Chitosan + 20% Lignin		Chitosan + 30% Lignin	
	Dry	Wet	Dry	Wet	Dry	Wet	Dry	Wet
State								
Strength, MPa	62 ± 5	27 ± 3	36 ± 3	25 ± 2	33 ± 4	25 ± 2	28 ± 1	22 ± 3
Breaking elongation, %	45 ± 10	101 ± 2	27 ± 5	157 ± 7	35 ± 5	159 ± 5	30 ± 7	155 ± 10

3.8. Studies of Biocompatibility

Human dermal fibroblasts were cultured on the chitosan, chitosan/lignin composite film matrices, and the cultural polystyrene surface (control surface). After cell attachment, the cells seeded on film matrices and the cultural polystyrene surface were incubated for four days in the culture medium at 37 °C in a humidified atmosphere containing 5% of CO₂. The cell viability and proliferation were evaluated using SEM and the MTT tests.

The SEM studies showed that in comparison with the pure chitosan matrix, the composite matrix containing lignin was more efficient in providing spreading and regular growth of dermal fibroblasts (Figure 7).

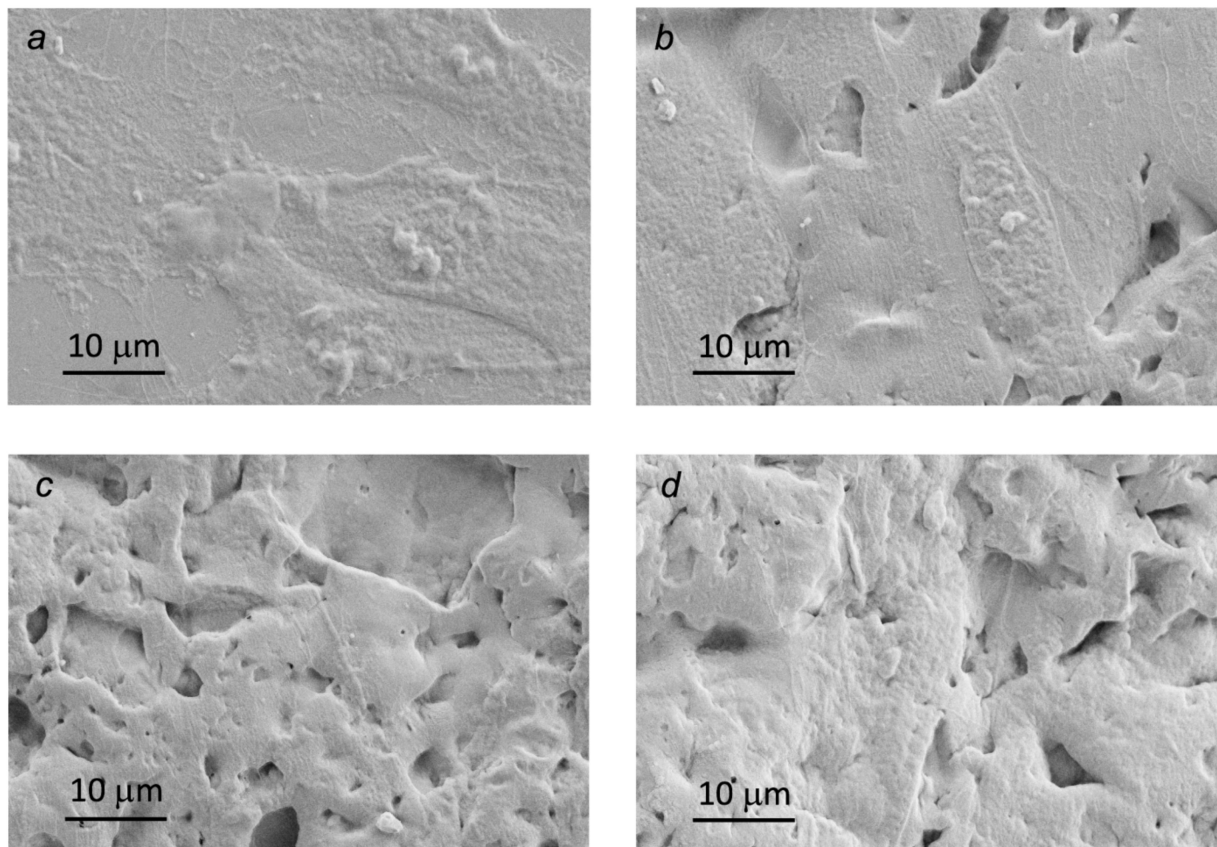


Figure 7. SEM images of human dermal fibroblasts grown of the surface of pure chitosan matrix (a) and composite matrix containing 10% of lignin (b), (c) 20% of lignin, and (d) 30% of lignin after 4 days of cultivation.

The MTT test revealed that the samples containing 20 and 30% of lignin matrices facilitated higher cell proliferative activity than the pure chitosan matrix. The difference was found statistically reliable and increased with increasing lignin concentration (Figure 8).

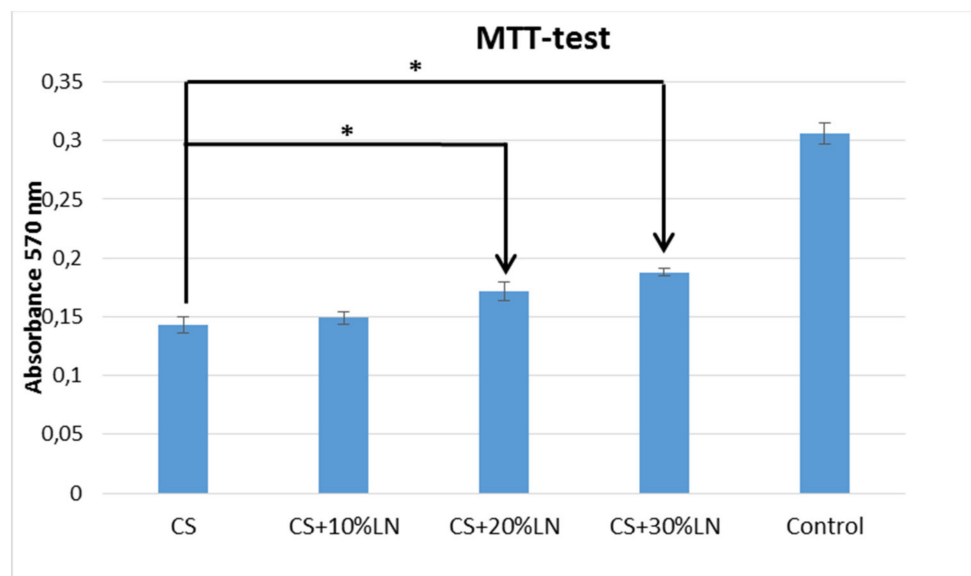


Figure 8. The viability and proliferation of human dermal fibroblasts on surfaces of film matrices and cultural polystyrene surface (control) as determined by MTT assay. The MTT test involved human dermal fibroblasts cultured on the surface of the chitosan-based nanocomposite matrices with the addition of 0, 10, 20, and 30 wt% lignin for 4 days. Cells cultivated on polystyrene surface served as control. Here, the optical density correlates with the number of viable cells. * $p < 0.05$.

4. Discussion

It is known that the bioactivity of a composite material depends on the nature of its components, the physical and chemical interactions between these components, its surface characteristics, and the physico-chemical and mechanical properties of this composite.

It was demonstrated here that the introducing of lignin into the chitosan matrix makes it possible to obtain composite systems possessing bioactivity (facilitating cell growth) and showing sufficient mechanical strength and elasticity for operating in air and in a liquid medium.

The DMA results revealed that chitosan and lignin are thermodynamically incompatible polymers [40]. Structurization in the mixtures of thermodynamically incompatible polymers occurred at micro- and macrolevels. At the macrolevel, either a dispersed system or interpenetrating structure was formed, depending on the ratio among the initial components, viscosity, molecular mass distribution, and preparation technique. A special feature of these systems was that they not only retained the properties of the initial components but also may acquire new properties not inherent to any of the pure components. This behavior may be related to the formation of a microstructure with relatively loose packing of macromolecules at the phase interface among thermodynamically incompatible polymers [41,42].

Some understanding of the interaction between chitosan and lignin can be gained from the analysis of the IR spectra presented in Figure 2, which implied that a salt was formed between the protonated amino group of chitosan and the carboxylic group of lignin. The formation of these bonds led to the appearance of a crosslinked framework carrying the main mechanical load. The data of X-ray structural analysis demonstrated that the introduction of amorphous lignin did not result in considerable changes in the crystalline structure of chitosan. As seen in the X-ray diffractograms, the peak corresponding to the crystalline phase of chitosan was retained in the patterns of composites. However, the intensity of this peak decreased in the diffractograms of composites (in comparison to that of the initial chitosan). It can be assumed that two components of this film (chitosan and lignin) form the two-phase interpenetrating lamellar structure [40,43] oriented along the film surface (2D). The formation of a bond between the components could take place on the surfaces of interphase layers. The amount of bonds formed between chitosan and

lignin did not depend on the percentage of introduced lignin; it was equal in all the cases and was determined by the amount of reactive protonated amino groups in chitosan. This hypothesis is confirmed by the results of mechanical tests. The mechanical characteristics of the composites both in the dry and wet states deteriorated in comparison to those of the initial chitosan film. At the same time, the values of mechanical strength, modulus and breaking elongation for all composites were virtually similar independently of the amount of introduced lignin. The wet composite films demonstrated considerably higher breaking elongation values in comparison with both the dry samples and (pure) samples chitosan [42]. The breaking elongation values for all composites were similar and lay within the normal range of experimental results. Within the framework of the model discussed above, we can suppose that the presence of lignin in the composite restricts the swelling of chitosan in a liquid medium, and the bonds formed between components play a role in an elastic framework. This framework allowed for swollen chitosan phase to deform (stretch) during film extension, but prevented its disruption up to considerable breaking elongation (as opposed to that of pure chitosan film). It should be noted that during swelling, the (planar) area of the films changed predominantly, while the increase in thickness was relatively small; this fact may also indicate that in chitosan/lignin film, a 2D structure is mainly formed [44].

The swelling kinetics of chitosan and composite films were investigated in water and in physiological solution. The obtained results showed that in both solutions, the initial chitosan film had the highest swelling degree, and the lowest swelling degree was found for the composite containing 10% of lignin. This result can be explained by the fact that the introduction of lignin caused the appearance of a hydrated chitosan polymorph, which is characterized by a looser packing as compared to the anhydrous form [40,45,46]. The introduction of 10% of lignin did not disturb the chitosan structure and dense packaging of macromolecules. Lignin was uniformly dispersed between the layers of chitosan [21] and prevented the penetration of solvent molecules to the chitosan phase, which, here, resulted in a decrease in the swelling degree of the samples containing 10% of lignin in comparison with that of the initial chitosan film. A further increase in the lignin content in the composites until 20 and 30% led to the separation of chitosan chains due to the formation of the lignin phase inside the film and amorphization of the samples [47]. As a consequence, the internal structure of the films became “loosened”, and the surface structure underwent changes. The surface acquired a pronounced texture and porosity, which explained the increased swelling of the composites containing high amounts of lignin. The abovementioned results are in a good agreement with the X-ray structural analysis data.

The formation of an ordered structure was confirmed by an increase in the intensity of the peaks related to the glycoside bonds in the IR spectrum of the sample containing 10% of lignin. When 20 or 30% of lignin was introduced into the chitosan matrix, the packing of macromolecules on the phase interface became looser, which led to more pronounced swelling of these composites both in water and in physiological solution [35].

The SEM images revealed that the introducing of lignin resulted in considerable changes in the chitosan surface morphology. The surface of lignin-containing composites was porous and textured. With an increasing lignin content in the composite, the amount of pores increased, and the surface texture became more pronounced. The changes in the surface morphology caused by the introducing of lignin into the chitosan matrix were also confirmed by the AFM data.

Previous research has shown that the biocompatibility and bioactivity of a composite material depend on the nature of components, the physical and chemical interactions between them, as well as the surface properties of the matrix prepared on the base of this composite [48,49]. The modification of chitosan matrices with lignin makes it possible to obtain composite systems characterized by good mechanical strength and elasticity sufficient for operation in the dry and wet states, which is necessary for sterilization, manipulation, and cell cultivation. Due to their textured surface and developed porosity,

these materials can be used as matrices for cell cultivation. An increase in the lignin content possibly leads to the appearance of more significant porosity and an enhanced texture, thus increasing the surface area of a matrix suitable for cell growth.

To summarize, we obtained biocompatible and bioactive material systems based on the composites containing natural polymers (chitosan and lignin), which may find application in tissue engineering.

Author Contributions: Conceptualization, E.R.; Methodology, E.R.; E.D., N.S.; Validation, V.Y.; Investigation, N.S.; M.S.; V.S.; K.K., E.D.; E.V., E.I., T.M.; K.M.; Writing—Original Draft Preparation, E.R.; E.D.; M.S.; N.S.; Writing—Review & Editing, E.R.; M.K.; E.D.; M.S.; Supervision, V.Y. All authors have read and agreed to the published version of the manuscript.

Funding: This research was funded by RSF, grant number 19-73-30003.

Institutional Review Board Statement: Not applicable.

Informed Consent Statement: Not applicable.

Data Availability Statement: Not applicable.

Conflicts of Interest: The authors declare no conflict of interest.

References

1. Lee, D.; Heo, D.N.; Lee, S.J.; Heo, M.; Kim, J.; Choi, S.; Park, H.-K.; Park, Y.G.; Lim, H.-N.; Kwon, I.K. Poly(lactide-co-glycolide) nanofibrous scaffolds chemically coated with gold-nanoparticles as osteoinductive agents for osteogenesis. *Appl. Surf. Sci.* **2018**, *432*, 300. [[CrossRef](#)]
2. Amani, H.; Mostafavi, E.; Arzaghi, H.; Davaran, S.; Akbarzadeh, A.; Akhavan, O.; Pazoki-Toroudi, H.; Webster, T.J. Three-dimensional graphene foams: Synthesis, properties, biocompatibility, biodegradability, and applications in tissue engineering. *ACS Biomater. Sci. Eng.* **2019**, *5*, 193. [[CrossRef](#)]
3. Majeti, N.V.; Kumar, R. A Review of Chitin and Chitosan Applications. *React. Funct. Polym.* **2000**, *46*, 1–27. [[CrossRef](#)]
4. Rao, G.; Bharathi, P.; Akila, R.M. A comprehensive review on biopolymers. *Sci. Revs. Chem. Commun.* **2014**, *4*, 61–68.
5. Dobrovolskaya, I.P.; Yudin, V.E.; Popryadukhin, P.V.; Ivan'kova, E.M. *Polymer Scaffolds for Tissue Engineering*; Mediapapir: Saint-Petersburg, Russia, 2018.
6. Sokolova, M.P.; Smirnov, M.A.; Samarov, A.A.; Bobrova, N.V.; Vorobiov, V.K.; Popova, E.N.; Filippova, E.; Geydt, P.; Lahderanta, E.; Toikka, A.M. Plasticizing of chitosan films with deep eutectic mixture of malonic acid and choline chloride. *Carbohydr. Polym.* **2018**, *197*, 548–557. [[CrossRef](#)] [[PubMed](#)]
7. Dufresne, A.; Sabu, T.; Laly, A.P. *Biopolymer Nanocomposites: Processing, Properties, and Applications*; Wiley: San Francisco, CA, USA, 2013.
8. Prateepchanachai, S.; Thakhiewb, W.; Devahastinc, S.; Soponronnarit, S. Mechanical properties improvement of chitosan films via the use of plasticizer, charge modifying agent and film solution homogenization. *Carbohydr. Polym.* **2017**, *174*, 253–261. [[CrossRef](#)] [[PubMed](#)]
9. Ye, Y.; Dan, C.; Zeng, W.H.; Lin, H.; Dan, N.H. Miscibility studies on the blends of collagen/chitosan by dilute solution viscometry. *Eur. Polym. J.* **2007**, *43*, 2066. [[CrossRef](#)]
10. Mathew, S.; Brahmakumar, M.; Abraham, E. Microstructural imaging and characterization of the mechanical, chemical, thermal, and swelling properties of starch-chitosan blend films. *Biopolymers* **2006**, *82*, 176–187. [[CrossRef](#)] [[PubMed](#)]
11. Smirnova, N.; Kolbe, K.; Dresvyanina, E.; Grebennikov, S.; Dobrovolskaya, I.; Yudin, V.; Luxbacher, T.; Morganti, P. Effect of Chitin Nanofibrils on Biocompatibility and Bioactivity of the Chitosan-Based Composite Film Matrix Intended for Tissue Engineering. *Materials* **2019**, *12*, 1874. [[CrossRef](#)]
12. Di Martino, A.; Sittigerc, M.; Risbud, M.V. Chitosan: A versatile biopolymer for orthopaedic tissue-engineering. *Biomaterials* **2005**, *26*, 5983. [[CrossRef](#)]
13. Pogorielov, M.V.; Sikora, V.Z. Chitosan as a hemostatic agent: Current state. *Eur. J. Med. Ser. B* **2015**, *2*, 24. [[CrossRef](#)]
14. Kumar Thakur, V.; Kumar Thakur, M. Recent Advances in Graft Copolymerization and Applications of Chitosan: A Review. *ACS Sustain. Chem. Eng.* **2014**, *2*, 2637. [[CrossRef](#)]
15. Pinheiro, A.C.; Bourbon, A.I.; Quintas, M.A.C.; Coimbra, M.A.; Vicente, A.A. K-carrageenan/chitosan nanolayered coating for controlled release of a model bioactive compound. *Innov. Food Sci. Emerg. Technol.* **2012**, *16*, 227. [[CrossRef](#)]
16. Musilová, L.; Mráček, A.; Kovalčík, A.; Smolka, P.; Minařík, A.; Humpolíček, P.; Vícha, R.; Ponížil, P. Hyaluronan hydrogels modified by glycinated Kraft lignin: Morphology, swelling, viscoelastic properties and biocompatibility. *Carbohydr. Polym.* **2018**, *181*, 394. [[CrossRef](#)] [[PubMed](#)]
17. Núñez-Flores, R.; Giménez, B.; Fernández-Martín, F.; López-Caballero, M.E.; Montero, M.P.; Gómez-Guillén, M.C. Physical and functional characterization of active fish gelatin films incorporated with lignin. *Food Hydrocoll.* **2013**, *30*, 163. [[CrossRef](#)]

18. Spiridon, I.; Tanase, C.E. Design, characterization and preliminary biological evaluation of new lignin-PLA biocomposites. *Int. J. Biol. Macromol.* **2018**, *114*, 855. [[CrossRef](#)]
19. Pettersen, R.C. The chemical composition of wood. *Chem. Solid Wood* **1984**, *207*, 57.
20. Dallmeyer, I.; Chowdhury, S.; Kadla, J.F. Preparation and Characterization of Kraft Lignin-Based Moisture-Responsive Films with Reversible Shape-Change Capability. *Biomacromolecules* **2013**, *14*, 7. [[CrossRef](#)]
21. Crouvisier-Uriona, K.; Lagorce-Tachona, A.; Lauquina, C.; Wincklera, P.; Tongdeesoontornb, W.; Domenekc, S.; Debeauforta, F.; Karbowiaka, T. Impact of the homogenization process on the structure and antioxidant properties of chitosan-lignin composite films. *Food Chem.* **2017**, *236*, 120. [[CrossRef](#)]
22. Chen, L.; Tang, C.; Ning, N.; Wang, C.; Fu, Q.; Zngang, Q. Preparation and properties of chitosan/lignin composite films. *Chin. J. Polym. Sci.* **2009**, *27*, 739. [[CrossRef](#)]
23. Nair, V.; Panigrahy, R.; Vinu, R. Development of Novel Chitosan-Lignin Composites for Adsorption of Dyes and Metal Ions from Wastewater. *Chem. Eng. J.* **2014**, *254*, 491. [[CrossRef](#)]
24. Sudheer, R.; Dutta, P.K.; Mehrotra, G.K. Lignin Incorporated Antimicrobial Chitosan Film for Food Packaging Application. *J. Polym. Mater.* **2017**, *34*, 171.
25. Volkova, N.; Ibrahimia, V.; Hatti-Kaul, R.; Wadsö, L. Water sorption isotherms of Kraft lignin and its composites. *Carbohydr. Polym.* **2012**, *87*, 1817. [[CrossRef](#)]
26. Naseem, A.; Muhammad, N.; Muhammad, Z.; Muhammad, K.; Ejaz, A.W. Effect of consortium of plant growth promoting and compost inhabiting bacteria on physicochemical changes and defense response of maize in fungus infested soil. *Pak. J. Agric. Sci.* **2016**, *53*, 59. [[CrossRef](#)]
27. Krutov, S.; Evtuguin, D.; Ipatova, E.; Santos, S.; Sazanov, Y. Modification of acid hydrolysis lignin for value-added applications by micronization followed by hydrothermal alkaline treatment. *Holzforchung* **2015**, *69*, 761–768. [[CrossRef](#)]
28. Kosyakova, D.; Ipatova, E.; Krutov, S.; Ul'yanovskii, N.; Pikovskoi, I. Study of Products of the Alkaline Decomposition of Hydrolysis Lignin by Atmospheric Pressure Photoionization High-Resolution Mass Spectrometry. *Anal. Chem.* **2017**, *72*, 1396–1403. [[CrossRef](#)]
29. Lawrence, E. *Nielsen, L.E. Mechanical Properties of Polymers and Composites*; CRC Press: Boca Raton, FL, USA, 1974.
30. Dresvyanina, E.N.; Dobrovol'skaya, I.P.; Yudin, V.E.; Smirnov, V.E.; Popova, E.N.; Vlasova, E.N. Thermal properties of salt and base forms of chitosan. *Polym. Sci. Ser. A* **2018**, *60*, 179–183. [[CrossRef](#)]
31. Smirnova, V.E.; Dresvyanina, E.N.; Popova, E.N.; Saprykina, N.N.; Yudin, V.E.; Kolbe, K.A. Thermomechanical analysis of composite films based on chitosan and chitin nanofibrils. *Russ. J. Appl. Chem.* **2019**, *92*, 1506. [[CrossRef](#)]
32. Narimane, M.-B.; De Hélène, B.; Christophe, V.; Fabrice, A. Physico-chemical, thermal, and mechanical approaches for the characterization of solubilized and solid state chitosans. *J. Appl. Polym. Sci.* **2014**, *131*, 46.
33. Zhao, J.; Han, W.; Chen, H.; Tu, M.; Zeng, R.; Shi, Y.; Cha, Z.; Zhou, C. Preparation, structure and crystallinity of chitosan nano-fibers by a solid-liquid phase separation technique. *Carbohydr. Polym.* **2011**, *83*, 1541. [[CrossRef](#)]
34. Vural, D.; Smithac, J.C.; Petridis, L. Dynamics of the lignin glass transition. *Phys. Chem. Chem. Phys.* **2018**, *20*, 20504–20512. [[CrossRef](#)]
35. Brugnerotto, J.; Lizardi, J.; Goycoolea, F.M.; Mona, L.W.A.; Desbrieres, J.; Rinaudo, M. An infrared investigation in relation with chitin and chitosan characterization. *Polymer* **2001**, *42*, 3569. [[CrossRef](#)]
36. Van de Velde, K.; Kiekens, P. Structure analysis and degree of substitution of chitin, chitosan and dibutylchitin by FT-IR spectroscopy and solid state ¹³C NMR. *Carbohydr. Polym.* **2004**, *58*, 409. [[CrossRef](#)]
37. Ageev, E.P.; Matushkina, N.N.; Gerasimov, V.I.; Zezin, S.B.; Vikhoreva, G.A.; Zotkin, M.A.; Obolonkova, E.S. Structure and transport behavior of heat-treated chitosan films. *Polym. Sci. Ser. A* **2004**, *46*, 1245.
38. Ogawa, K.; Yui, T.; Miya, M. Dependence on the Preparation Procedure of the Polymorphism and Crystallinity of Chitosan Membranes. *Biosci. Biotechnol. Biochem.* **1992**, *56*, 858–862. [[CrossRef](#)] [[PubMed](#)]
39. Ogawa, K.; Yui, T. Crystallinity of Partially N-Acetylated Chitosans. *Biosci. Biotechnol. Biochem.* **1993**, *57*, 1466–1469. [[CrossRef](#)]
40. Takara, E.A.; Marchese, J.; Ochoa, N. NaOH treatment of chitosan films: Impact on macromolecular structure and film properties. *Carbohydr. Polym.* **2015**, *132*, 25–30. [[CrossRef](#)] [[PubMed](#)]
41. Mochalova, A.E.; Nikishchenkova, L.V.; Smirnova, N.N.; Smirnova, L.A. Thermodynamic properties of chitosan-based hydrogels in the range 0–350 K. *Polym. Sci. Ser. B* **2007**, *49*, 42–46. [[CrossRef](#)]
42. Mogonov, D.M.; Ayurova, O.Z.; Stelmakh, S.A.; Ochirov, O.S.; Tkacheva, N.I.; Morozov, S.V. Thermodynamic compatibility of polymer blends. *Appl. Solid State Chem.* **2018**, *4*, 126–143. [[CrossRef](#)]
43. Kumirska, J.; Czerwicka, M.; Kaczynski, Z.; Bychowska, A.; Brzozowski, K.; Thöming, J.; Stepnowski, P. Application of Spectroscopic Methods for Structural Analysis of Chitin and Chitosan. *Mar. Drugs* **2010**, *8*, 1567–1636. [[CrossRef](#)] [[PubMed](#)]
44. Demarger-Andre, S.; Domard, A. Chitosan carboxylic acid salts in solution and in the solid state. *Carbohydr. Polym.* **1994**, *23*, 211–219. [[CrossRef](#)]
45. Kawada, J.; Yui, T.; Okuyama, K.; Ogawa, K. Crystalline Behavior of Chitosan Organic Acid Salts. *Biosci. Biotechnol. Biochem.* **2001**, *65*, 2542–2547. [[CrossRef](#)] [[PubMed](#)]
46. Baklagina, Y.G.; Klechkovskaya, V.V.; Kononova, S.V.; Petrova, V.A.; Poshina, D.N.; Orekhov, A.S.; Skorik, Y.A. Polymorphic Modifications of Chitosan. *Crystallogr. Rep.* **2018**, *63*, 303–313. [[CrossRef](#)]

-
47. Smirnov, M.; Nikolaeva, A.; Vorobiov, V.; Bobrova, N.V.; Abalov, I.; Smirnov, A.; Sokolova, M. Ionic Conductivity and Structure of Chitosan Films Modified with Lactic Acid-Choline Chloride NADES. *Polymers* **2020**, *12*, 350. [[CrossRef](#)] [[PubMed](#)]
 48. Amani, H.; Arzaghi, H.; Bayandori, M.; Shiralizadeh Dezfuli, A.; Pazoki-Toroudi, H.; Shafiee, A.; Moradi, L. Controlling Cell Behavior through the Design of Biomaterial Surfaces: A Focus on Surface Modification Techniques. *Adv. Mater. Interfaces* **2019**, *6*, 1900572. [[CrossRef](#)]
 49. Rex, C.-C.; Wang, C.; Hsieh, M.-C.; Leea, T.-M. Effects of nanometric roughness on surface properties and fibroblast's initial cytocompatibilities of Ti₆Al₄V. *Biointerphases* **2011**, *6*, 87–97. [[CrossRef](#)]